Janus Particles

DOI: 10.1002/anie.201007519

Inorganic Janus Nanosheets**

*Fuxin Liang, Ke Shen, Xiaozhong Qu, Chengliang Zhang, Qian Wang, Jiaoli Li, Jiguang Liu, and Zhenzhong Yang**

Janus objects have two different compositions compartmentalized onto the same surface, and have shown some unique performance properties. They have gained growing interest for both academic and industrial considerations.[1,2] For example, some new complex superstructures can be created as building blocks because of their directional interaction and amphiphilicity.[3–5] As solid surfactants, Janus particles can stabilize an emulsion more effectively than their homogeneous counterparts in Pickering emulsions.[3] The currently reported morphologies mainly focus on particulate and rod forms;[2] Janus platelets, especially nanosheets, deserve more attention because of their highly anisotropic shape as well as their chemistry. Compared with Janus spheres, rotation of Janus platelets at an interface is greatly restricted, thus making the emulsion more stable as the planar configuration facilitates their favorable orientation thereby.[4] It is significant to develop methods for the large-scale synthesis of such Janus platelets, especially nanosheets. Recently, nanometer-sized polymeric Janus disks have been synthesized by cross-linking those supramolecular structures from block copolymers.[5] The copolymers should have specific chain structure. Polymeric disks usually swell and thus deform in the presence of solvents. The synthesis of robust inorganic Janus nanosheets is urgently required. Although a method is proposed to produce inorganic Janus platelets on a large scale by crushing modified glass hollow spheres, the thicknesses of the platelets are over micrometers and their composition is ill-defined.[6] Inorganic Janus sheets have been recently prepared on the basis of etching substrates, which have displayed promising performance.[7] In particular, multistep etching of silicon produces Janus nanosheets. "Dry" liquid droplets in air are stable with such Janus nanosheets loaded at the interface. However, in principle, the large-scale synthesis of inorganic Janus nanosheets is thereby impossible.

Herein, we report a facile approach for large-scale production of inorganic Janus nanosheets by crushing silica Janus hollow spheres (Scheme 1). The silica Janus hollow spheres are synthesized by a self-assembled sol–gel process at an emulsion interface to form a shell.[8] The shell thickness is tunable to within nanometers. As an example, the hydrophilic amine- and hydrophobic phenyl-terminated species self-assemble at the interface, which face the external aqueous and the internal oil core phases, respectively. By favorable growth of other materials onto the desired side, the composition and microstructure of the Janus nanosheets can be greatly extended, and some new additional features can be introduced. The Janus nanosheets can serve as solid surfactants to stabilize emulsion droplets, and many chemical spills can be collected thereby.

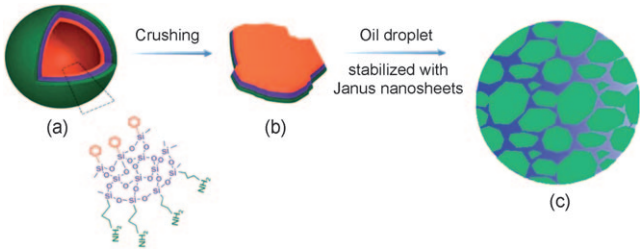

Scheme 1. Fabrication of silica Janus nanosheets and their Janus performance as a solid surfactant. An oil/silica core–shell structure forms by a self-assembled sol–gel process at the emulsion interface. Hydrophilic amine- and hydrophobic phenyl-terminated species self-assemble at the interface and form a robust shell, facing the external aqueous phase and internal oil phase, respectively. The thickness of the shell can be tuned to within nanometers. a) After dissolution of the core, silica Janus hollow spheres form. b) By crushing the silica Janus hollow spheres, the corresponding silica Janus nanosheets are derived. c) The Janus nanosheets can be used as a solid surfactant to emulsify immiscible liquid mixtures.

Under acidic condition, for example pH 2.5, the sol–gel process predominantly occurs at the interface to form a smooth silica shell.[9] The amine group becomes positively charged, facilitating the species to face the external aqueous phase and the phenyl-terminated species face the internal oil phase. With a prolonged sol–gel process, the siliceous species are cross-linked at the interface. Micrometer-sized core/shell structures eventually form with the crystallized oil phase distinguished upon cooling (Figure S1a in the Supporting Information). The corresponding Janus hollow spheres form after the oil core is dissolved (Figure S1b). The Janus hollow spheres were further crushed into Janus nanosheets by colloid milling (Figure 1a). Both sides of the Janus nanosheets are smooth. The cross-sectional dimension of the nanosheets is tunable by controlling both the mill spacing between the rotators and milling time. For example, when the milling spacing is fixed at 2 μm, with the increase in milling time, the

[*] F. X. Liang, K. Shen, Dr. X. Z. Qu, Dr. C. L. Zhang, Dr. Q. Wang, Dr. J. L. Li, Dr. J. G. Liu, Prof. Z. Z. Yang
State Key Laboratory of Polymer Physics and Chemistry
Institute of Chemistry, Chinese Academy of Sciences
Beijing, 100190 (China)
Fax: (+86) 10-6255-9373
E-mail: yangzz@iccas.ac.cn
Homepage: http://yangzz.iccas.ac.cn/

[**] We thank Prof. Zhibing Hu of the University of North Texas and Prof. Yunfeng Lu of UCLA for helpful discussions. This work was supported by the NSF of China (50733004, 50821062, and 50973121), CAS, and MOST.

Supporting information for this article is available on the WWW under http://dx.doi.org/10.1002/anie.201007519.

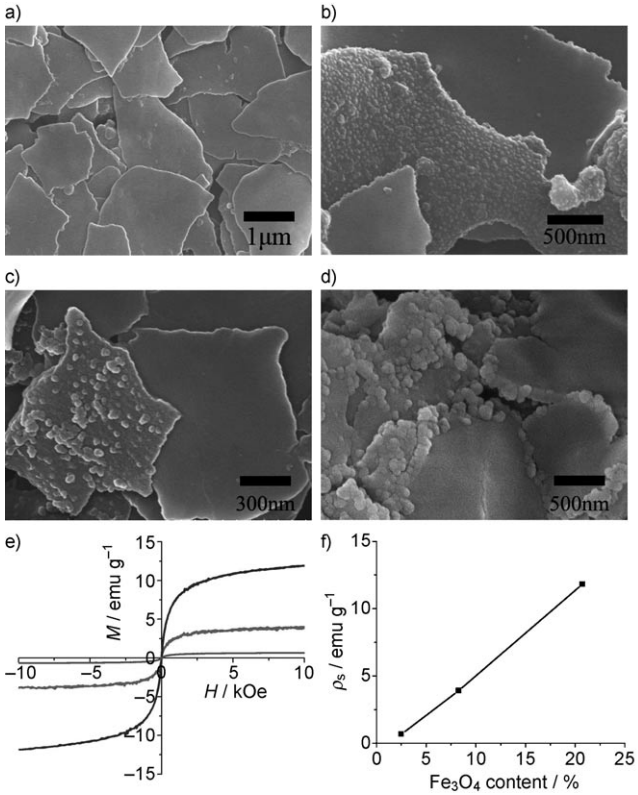

Figure 1. Some representative Janus nanosheets: a) Janus nanosheets after the parent hollow spheres were crushed by colloid milling; b) Janus nanosheets with the sulfonated PS nanoparticles selectively labeled (about 30 nm in diameter) on the amine-terminated side; c) the Janus nanosheets after being sulfonated and subsequently labeled with amine-capped SiO_2 nanoparticles (30–50 nm in diameter) selectively on one side; d) Janus nanosheets with the trisodium citrate capped Fe_3O_4 nanoparticles selectively conjugated onto the amine-terminated side (sample M2); e) hysteresis loop of the Fe_3O_4-modified Janus nanosheets at room temperature; f) magnetic saturation dependence on the Fe_3O_4 nanoparticle content.

hollow spheres are eventually crushed to nanosheets. At the intermediate milling stage, hollow spheres and the nanosheets coexist (Figure S2). The cross-sectional dimension of the nanosheets is micrometer-sized and has a broad distribution. To decrease cross-section dimension of the nanosheets further, the spacing between the rotators must be decreased (Figure S3). However, the shape of the nanosheets becomes ill-defined. The thickness of the nanosheets is not influenced by the milling process. The thickness of representative Janus nanosheets (as shown in Figure 1 a) was measured by atomic force microscopy (AFM) to be 65 nm, which is equivalent to the shell thickness of the parent hollow spheres.[8] The fluctuation of the height image is rather small, revealing that the thickness of the nanosheets is relatively uniform. A cross-sectional TEM image of the nanosheets shows that the thickness of the nanosheets is uniform (Figure S4). The thickness of the nanosheets is tunable by varying the precursor content in the oil phase for example from 24 nm at 5.5 wt% to 95 nm at 36.9 wt%.[8]

The chemistry of the Janus nanosheets was characterized by FTIR and energy-dispersive X-ray (EDX) spectroscopy (Figure S5). The peak centered at 3400 cm^{-1} reveals the presence of an amine group. The characteristic peaks between 1620–1450 cm^{-1} and at 3060 cm^{-1} show the presence of a phenyl group. The peak centered at 700 cm^{-1} is assigned to monosubstituted benzene. The EDX results show the presence of the element N, corresponding to the amine group. To further confirm the location of the amine group on one side of the nanosheets, we designed other experiments. Anionic sulfonated polystyrene (sPS) nanoparticles about 30 nm in diameter were used to selectively label the amine-terminated region by electrostatic interaction. One side becomes coarser while the other side remains smooth (Figure 1 b). Another relatively direct piece of evidence is provided. The polymer benzaldehyde-terminated poly(ethylene glycol) at the chain end (PEG-CHO) was used to treat the amine group covalently and selectively through a Schiff base reaction (Figure S6). Similarly, only one side becomes coarsened after being conjugated with PEG-CHO. The results confirm that one side contains the amine group whereas the other side contains no amine groups. To reveal the presence of the phenyl group on the other side, the Janus nanosheets were treated with concentrated sulfuric acid to selectively sulfonate the phenyl group (Figure S7a). The nanosheets become dispersible in water but not in oil phases. The presence of the element S was detected in the EDX spectrum (Figure S7b), confirming the sulfonation of phenyl group. After introduction of the amine group capped SiO_2 nanoparticles to the aqueous dispersion, one side becomes coarsened while the other side remains smooth (Figure 1 c). These results conclusively confirm that the nanosheets are terminated with phenyl and amine groups on the two individual sides. Similarly, trisodium citrate capped paramagnetic Fe_3O_4 nanoparticles were preferentially conjugated onto the amine-terminated side to render a magnetic response (Figure 1 d). The loading amount (Figure S8), and thus the magnetic response capability, is tunable (Figure 1 e). Magnetic saturation was measured by using vibrating sample magnetometer and is proportional to the Fe_3O_4 nanoparticle content (Figure 1 f).

We will now demonstrate the collection of chemical spills by using the Janus nanosheets as solid surfactants by emulsifying immiscible liquids to form stable emulsions. Toluene and water are typically immiscible. Methyl orange was added to the bottom water phase for easy observation. In the presence of the Janus nanosheets (as shown in Figure 1 a), a stable toluene-in-water emulsion forms when water is present in a suitable proportion, for example 33% (Figure 2 a). The continuous aqueous phase is electrically conductive. The droplet size ranges within 0.1–0.3 mm (Figure 2 b). The as-prepared emulsion remains stable for at least 6 months. The emulsification essentially originates from the amphiphilicity of the Janus nanosheets rather than a Pickering effect, since the Janus nanosheets can be well dispersed both in water and oil phases (Figure S9). For example, in the case in water, the Janus nanosheets can stack into a back-to-back superstructure with the amine group terminated side exposed to the aqueous phase (Figure S10), similar to hydrophobic association of amphiphilic polymers. This is consistent with amphiphilicity of the Janus nanosheets. To observe the

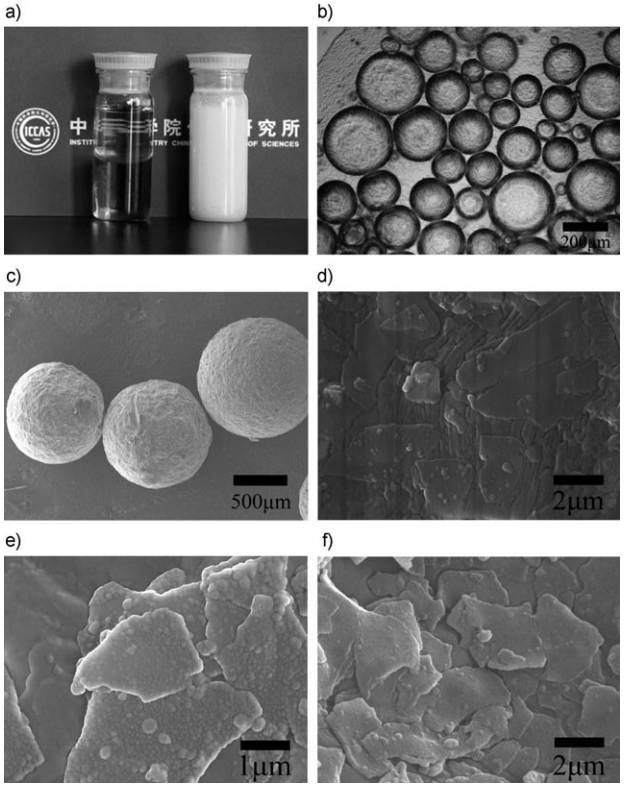

Figure 2. Emulsification of representative immiscible liquid mixtures with the Janus nanosheets: a) left: immiscible mixture of toluene (top) and water (bottom); right: toluene-in-water emulsion stabilized with the Janus nanosheets; b) optical microscopy image of the toluene-in-water emulsion; c) SEM image of the paraffin (T_m: 52–54 °C) droplets stabilized with the Janus nanosheets; the weight ratio of Janus nanosheets/paraffin/water is 0.005:1.5:2.5 (Janus nanosheet content 0.12 wt %); d,e) SEM image of the Janus nanosheets on frozen paraffin droplets of the sample as shown in Figure 2c before (d) and after (e) sPS nanoparticles were selectively labeled onto the amine-terminated side; f) SEM image of the Janus nanosheets on the frozen paraffin droplets; the weight ratio of Janus nanosheets/paraffin/water is 0.025:1.5:2.5 (Janus nanosheet content 0.63 wt %).

orientation of the nanosheets at the interface, a melt paraffin (T_m: 52–54 °C) in water emulsion forms at high temperature. After the paraffin core is solidified upon cooling to room temperature, the orientation of the Janus nanosheets is frozen (Figure 2c). At a low nanosheet content level, for example of 0.12 wt %, the paraffin core surface is partially covered with a single layer of the nanosheets parallel onto the surface (Figure 2d). The element Si was detected in the EDX spectra (Figure S11) in the region covered with the Janus nanosheets, whereas no silicon was detected in the selected region without the Janus nanosheets. In between the nanosheets, the paraffin surface is naked and exposed to the aqueous phase. Upon absorbing the sPS nanoparticles, the exterior surface becomes coarse (Figure 2e), indicating that the amine-terminated side faces the aqueous phase. By increasing the Janus nanosheet content, the droplets become smaller (Figure S12), and the nanosheets begin to stack into multiple layers onto the surface (Figures 2f and S13). The droplets become larger with increasing oil content at a given Janus nanosheet content (Figure S14). Conversely, when water is a minor phase, for example 10 wt %, a water-in-toluene inverse emulsion forms. Besides immiscible aqueous mixtures, the Janus nanosheets can also emulsify nonaqueous immiscible mixtures, such as dimethylformamide/hexane systems.

While the example toluene-in-water emulsion (as shown in Figure 3a) flows through a porous mica membrane, water elutes and the toluene droplets are left. The volume of water

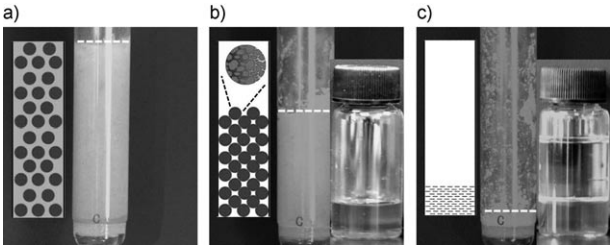

Figure 3. Oil/water separation from the emulsion stabilized with the Janus nanosheets: a) a toluene-in-water emulsion passing through a porous mica membrane (size of the sieve pores smaller than the droplets); b) water eluted while toluene droplets were preserved in air; c) toluene droplets coalesced and toluene eluted upon stirring.

in the eluate is almost the same as that in the mixture. As a result, the "dry" oil droplets are preserved in air rather than coalescencing (Figure 3b). This result indicates that the emulsions are rather stable with the Janus nanosheets. Upon stirring, the "dry" oil droplets coalesce and consequently almost all the oil elutes (Figure 3c). The nanosheets are left on the porous mica. Separation of each component was completed in the presence of the Janus nanosheets. It has been predicted that disk-shaped Janus particles can make emulsions more stable than their spherical counterparts because of their confined rotation.[4] Our process is valid for all the tested organic solvents, meaning that the method is general. Although some "dry" droplets can be obtained from Pickering emulsions by using non-Janus solid particles, their surface wettability should be specially tuned.[10] Although Janus spherical counterparts can emulsify more solvents, they cannot produce "dry" oil droplets, at least not so easily.[11] Simple calculations indicate that fewer disk-shaped particles can cover the same interfacial area than their spherical counterparts (Figure S15), meaning that the Janus nanosheets are more efficient to stabilize emulsions.

Additional performance, for example a magnetic response, can be imposed onto the Janus nanosheets. The Janus composite nanosheets with the Fe_3O_4 nanoparticles (intermediate content about 8 wt %) selectively conjugated onto the amine-terminated side can be manipulated with a magnet (Figure 4a). Upon applying a magnetic field to the toluene-in-water emulsion, the dispersed toluene droplets moves towards the magnet and are thereby collected (Figure 4b). While continuous water elutes, the toluene droplets are collected (Figure 4c). Upon stirring, the droplets coalesce and oil elutes. The Janus composite nanosheets can be collected and recycled for reuse by using the magnet (Figure 4d). We have demonstrated a general and easy approach to entrap oil from their surroundings, for example water by emulsification using Janus nanosheets, and subsequently to

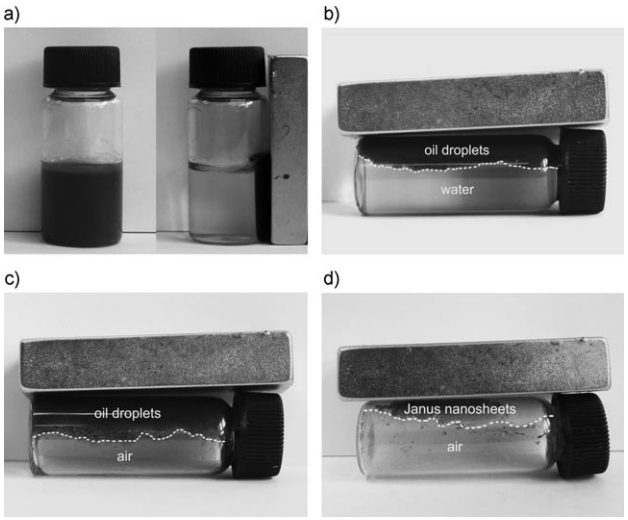

Figure 4. Magnetic manipulation of the emulsion stabilized with the paramagnetic Janus composite nanosheets: a) the paramagnetic Janus composite nanosheets (as shown in Figure 1 d) were dispersed in water, and could be driven using a magnet; b) a bottle was filled with an oil-in-water emulsion stabilized with the paramagnetic Janus nanosheets, and the oil droplets moved towards the magnet on the top of the bottle; c) water eluted when the bottle was opened, while oil droplets were collected by the magnet; d) oil eluted after the oil droplets coalesced upon stirring and the collected paramagnetic Janus nanosheets were dried and could be recycled.

collect the oil droplets from water by either filtration or magnetic manipulation. Upon stirring, the "dry" droplets coalesce and the trapped oil is released. The Janus nanosheets can be easily collected for reuse. The performance is promising for easily collecting oil or hazardous chemical spills.

In summary, a facile method is proposed for the fabrication of inorganic silica Janus nanosheets by crushing the corresponding parent Janus hollow spheres. The chemistry of the two sides is tunable. On one side, materials can be selectively grown to extend Janus nanosheets family. The Janus performance of the nanosheets was demonstrated by emulsifying immiscible liquids. Functionalized paramagnetic Janus composite nanosheets were derived by preferential growth of materials onto the amine-terminated side. Accordingly, the emulsion can be magnetically manipulated. By extending the method to form Janus hollow spheres by self-assembled materilization of an emulsion interface to other chemistry besides silica, it is expected to further tune composition and microstructure of the Janus hollow spheres and thus the nanosheets.

Received: November 30, 2010
Published online: February 11, 2011

Keywords: emulsions · Janus particles · nanosheets · silica · surfactants

[1] a) P. G. de Gennes, *Rev. Mod. Phys.* **1992**, *64*, 645 – 648; b) L. Hong, A. Cacciuto, E. Luijten, S. Granick, *Nano Lett.* **2006**, *6*, 2510 – 2514; c) H. Takei, N. Shimizu, *Langmuir* **1997**, *13*, 1865 – 1868; d) S. C. Glötzer, *Science* **2004**, *306*, 419 – 420; e) K. H. Roh, D. C. Martin, J. Lahann, *Nat. Mater.* **2005**, *4*, 759 – 763; f) D. Dendukuri, D. C. Pregibon, J. Collins, T. A. Hatton, P. S. Doyle, *Nat. Mater.* **2006**, *5*, 365 – 369.

[2] a) A. Perro, S. Reculusa, S. Ravaine, E. B. Bourgeat-Lami, E. Duguet, *J. Mater. Chem.* **2005**, *15*, 3745 – 3760; b) A. Walther, A. H. E. Müller, *Soft Matter* **2008**, *4*, 663 – 668.

[3] a) B. P. Binks, P. D. I. Fletcher, *Langmuir* **2001**, *17*, 4708 – 4710; b) N. Glaser, D. J. Adams, A. Boker, G. Krausch, *Langmuir* **2006**, *22*, 5227 – 5229.

[4] a) Y. Nonomura, S. Komura, K. Tsujii, *Langmuir* **2004**, *20*, 11821 – 11823; b) Y. Nonomura, S. Komura, K. Tsujii, *J. Phys. Chem. B* **2006**, *110*, 13124 – 13131.

[5] a) A. Walther, X. André, M. Drechsler, V. Abetz, A. H. E. Müller, *J. Am. Chem. Soc.* **2007**, *129*, 6187 – 6198; b) A. Walther, M. Hoffmannc, A. H. E. Müller, *Angew. Chem.* **2007**, *119*, 737 – 740; *Angew. Chem. Int. Ed.* **2007**, *46*, 723 – 726; c) A. Walther, K. Matussek, A. H. E. Müller, *ACS Nano* **2008**, *2*, 1167 – 1178; d) A. Walther, M. Drechsler, A. H. E. Müller, *Soft Matter* **2009**, *5*, 385 – 390.

[6] B. Gruning, U. Holtschmidt, G. Koerner, G. Rossmy, US 4,715,986, **1987**.

[7] a) J. R. Dorvee, A. M. Derfus, S. N. Bhatia, M. J. Sailor, *Nat. Mater.* **2004**, *3*, 896 – 899; b) M. A. Bucaro, P. R. Kolodner, J. A. Taylor, A. Sidorenko, J. Aizenberg, T. N. Krupenkin, *Langmuir* **2009**, *25*, 3876 – 3879.

[8] F. X. Liang, J. G. Liu, C. L. Zhang, X. Z. Qu, J. L. Li, Z. Z. Yang, *Chem. Commun.* **2011**, *47*, 1231 – 1233.

[9] C. Brinker, G. Scherer, *Sol–Gel Science: The Physics and Chemistry of Sol–Gel Processing*, Academic Press, San Diego, CA, **1990**, chap. 3, pp. 99 – 127.

[10] a) B. P. Binks, S. O. Lumsdon, *Langmuir* **2000**, *16*, 2539 – 2547; b) B. P. Binks, S. O. Lumsdon, *Langmuir* **2000**, *16*, 8622 – 8631; c) B. P. Binks, R. Murakami, *Nat. Mater.* **2006**, *5*, 865 – 869; d) V. O. Ikem, A. Menner, A. Bismarck, *Angew. Chem.* **2008**, *120*, 8401 – 8403; *Angew. Chem. Int. Ed.* **2008**, *47*, 8277 – 8279; e) Z. F. Li, T. Ming, J. F. Wang, T. Ngai, *Angew. Chem.* **2009**, *121*, 8642 – 8645; *Angew. Chem. Int. Ed.* **2009**, *48*, 8490 – 8493; f) S. Abend, N. Bonnke, U. Gutschner, G. Lagaly, *Colloid Polym. Sci.* **1998**, *276*, 730 – 737; g) Y. Nonomura, N. Kobayashi, *J. Colloid Interface Sci.* **2009**, *330*, 463 – 466.

[11] C. Tang, C. L. Zhang, J. G. Liu, X. Z. Qu, J. L. Li, Z. Z. Yang, *Macromolecules* **2010**, *43*, 5114 – 5120.

